

# Viologen Tweezers to Probe the Force of Individual Donor-Acceptor $\pi$ -Interactions

Damien Sluysmans<sup>1,2</sup>, Long Zhang<sup>2</sup>, Xuesong Li<sup>2</sup>, Amine Garci<sup>2</sup>, J. Fraser Stoddart<sup>2,3,4</sup>, Anne-Sophie Duwez<sup>1</sup>.

<sup>1</sup> Research Unit MolSys, NanoChem, University of Liege, Sart-Tilman, B6a, 4000 Liege, Belgium

<sup>2</sup> Department of Chemistry, Northwestern University, 2145 Sheridan Road, Evanston IL 60208-3113 USA

<sup>3</sup> Institute for Molecular Design and Synthesis, Tianjin University, Tianjin 300072, China

<sup>4</sup> School of Chemistry, University of New South Wales, Sydney, New South Wales 2052, Australia

**Keywords:** single-molecule force spectroscopy, donor-acceptor interaction,  $\pi$ -interactions, atomic force microscopy, viologen

Cover Art Caption:

A molecular tweezer is designed to probe the mechanical strength of donor-acceptor  $\pi$ -interactions. Single-molecule force spectroscopy experiments reveal a clear signature for the mechanical opening of a single tweezer. The quantification of the force of interaction, as presented here, is instrumental for the design of operational artificial molecular machines.

## ABSTRACT

Donor-acceptor (DA)  $\pi$ -interactions are weak attractive forces that are exploited widely in molecular and supramolecular chemistry. They have been characterized extensively by ensemble techniques, providing values for their energies that are useful for the design of soft materials. In order to implement motions or operations based on these DA  $\pi$ -interactions in wholly synthetic molecular machines, the mechanical strength and force associated with their out-of-equilibrium performance are the key parameters, in addition to their energies obtained at thermodynamic equilibrium. In this context, we have used single-molecule force spectroscopy as a non-equilibrium technique to determine the mechanical strength of individual DA  $\pi$ -interactions in solution. We designed and synthesized a molecular tweezer able to encapsulate  $\pi$ -donors and also demonstrating a precise opening extension. The mechanical breaking between viologen units— $\pi$ -acceptors commonly employed in mechanically interlocked molecules—and several  $\pi$ -donors afforded a characteristic force-distance signature, revealing to the opening of individual viologen tweezers with an unambiguous extension. Single-tweezer host-exchange experiments performed *in situ* demonstrated the sensitivity of the technique. This simple design could be exploited in quantifying the force of a large range of weak noncovalent bonding interactions as well as the potential work that molecular machines can generate at the single-molecule level.

## INTRODUCTION

Noncovalent bonding interactions are weak attractive forces that link different molecular entities or components.<sup>1-2</sup> These hydrophobic,  $\pi$ - and electrostatic interactions are all known to play key roles in the conformational stability and dynamics of biomacromolecules and biological molecular machines.<sup>3-4</sup> The action of many weak interactions in parallel results in high stabilities in proteins folds and in DNA double helices.<sup>4</sup> The ease of breaking a single noncovalent bonding interaction, compared to the breaking of covalent bonds can also be beneficial, leading to a fast response towards an external stimulus. Investigations of this kind have already been reported<sup>5-6</sup> for biological machines such as DNA polymerases, helicases, and other biomolecular motors. The fast dynamics of these molecular systems is based on the possibility of breaking weak interactions sequentially and recreating them following an alternative path or at another location in the molecule, leading to conformational changes and eventually to a task being performed. In parallel, the design of artificial molecular machines is now flourishing with many bio-inspired, wholly synthetic molecules.<sup>7-11</sup> These (supra)molecules are rationally designed to exhibit a well-defined motion of one part of their molecular structure, or the movement of one component relative to another. The increased interest in a new type of bond, the mechanical bond,<sup>12</sup> has led to a wide range of molecules able to demonstrate controlled motion at the nanoscale level. Mechanically interlocked molecules<sup>12</sup> (MIMs) can exploit weak noncovalent bonding interactions in their working domains to perform a precise task<sup>13</sup>, e.g., transport, catalysis, etc. Most of them are designed following template strategies, i.e., employing recognition units with high association constants.<sup>12</sup> For instance, many MIMs have been synthesized using  $\pi$ -interaction-based template-directed synthesis<sup>14</sup> and take advantage of this type of interaction for the controlled motion of one component in relation to the others.<sup>12</sup> This associative interaction between aromatic components

is stronger between electron-rich and electron-poor moieties— namely, donor-acceptor (D-A)  $\pi$ -interactions.<sup>15</sup>

Both biological and artificial molecular machines and motors require a source of energy to be driven away from their thermodynamic equilibrium, thus permitting an energetically-favored modification to perform a specific task.<sup>16-18</sup> Although artificial molecular machines are subjected to non-equilibrium thermodynamics,<sup>19</sup> their design principles are still based on equilibrium parameters such as association constants ( $K_a$  values) in solution. The application of these values remains acceptable as far as synthetic chemistry is concerned, but another vision arises when it comes to characterizing the operation and mechanical work performed by individual molecular machines in comparison with the performance of their biological counterparts.

In this context, single-molecule force spectroscopy techniques are imperative and have already demonstrated promising developments for the quantitative determination of the mechanical force and work generated by individual (supra)molecules.<sup>20-21</sup> Atomic force microscopy (AFM) in addition to optical and magnetic traps are powerful techniques to perform force spectroscopy experiments at the single-molecule level. Single-molecule force spectroscopy (SMFS) consists<sup>22</sup> in trapping a molecule of interest and in stretching it mechanically in a controlled manner in order to observe a specific event, e.g., a (co)conformational change, the breaking of an interaction, a mechanical resistance, etc. A wide range of molecules including biopolymers,<sup>23-24</sup> synthetic polymers,<sup>25</sup> biological molecular machines<sup>5,26-27</sup> and prototypes of artificial machines<sup>28-32</sup> has been studied using these techniques during the past three decades. All these investigations require a proper interfacing strategy to reach the single-molecule limit and probe the desired interaction or (co)conformation. To the best of our knowledge, the measurement of an individual donor-acceptor  $\pi$ -interaction has never been reported. Cutting-edge investigations in this domain

so far only include a series of multiple donor-acceptor  $\pi$ -interactions combined with hydrogen bonding.<sup>31-32</sup>

Here, we have developed a strategy to quantify the mechanical force required to break individual donor-acceptor  $\pi$ -interactions. The 4,4-bipyridinium (or viologen) dication has been selected as the  $\pi$ -acceptor, since it is one of the most commonly used, as part of the blue box, i.e., cyclobis(paraquat-*p*-phenylene).<sup>33</sup> Different  $\pi$ -donors were selected (dimethoxybiphenyl, DMBP; dimethoxynaphthalene, DMNP; diamionaphthalene, DANP) as well-known molecules involved in  $\pi$ -interactions.<sup>12</sup> The lack of specificity of such interactions prevents us from using the common molecular recognition experiments, e.g., antigen-antibody recognition. Instead, we designed a bis(viologen) unit, connected by a biphenylmethyl linker, to act as an electron-deficient molecular tweezer (Fig. 1A) able to encapsulate  $\pi$ -donors. The loop connecting both viologen units has been designed specifically to show a well-defined (co)conformational change large enough to be detected by AFM (details in SI). The interfacing for AFM-based SMFS experiments was completed using two poly(ethylene glycol) (PEG) chains ( $M_n = 2000 \text{ g}\cdot\text{mol}^{-1}$ ) at both ends of the viologen tweezer, allowing the physisorption to occur onto the surface and also onto the tip during the stretching experiments. This simple strategy does not require any covalent interactions with the AFM probe, given that we are probing weak noncovalent bonding interactions. During a standard experiment, the surface functionalized with the viologen tweezers is immersed in a solution containing  $\pi$ -donors and the AFM tip is pushed onto the surface to attach the PEG linker physically, following our previously described strategy<sup>28,29,34</sup> to anchor PEG linkers on AFM tips for SMFS experiments. Following this attachment, the molecule is stretched in a controlled manner (Fig. 1B) and the force required to open the viologen tweezer mechanically is measured.

## RESULTS AND DISCUSSION

### *Synthesis of the viologen tweezer for AFM interfacing*

The viologen tweezer used for AFM experiments was synthesized following the protocol described in the SI. Briefly, viologen units were attached to bis[4-(bromomethyl)phenyl]methane to create a loop long enough to detect the viologen tweezer opening by AFM. The AFM interfacing was facilitated by clicking (CuAAC) modified PEG chains onto both ends of the viologen tweezer. The product was purified and characterized by  $^1\text{H}$  NMR and  $^{13}\text{C}$  NMR spectroscopies.

### *Promoting single-molecule attachment*

The viologen tweezers were drop-casted onto a mica surface (detailed protocol in the SI). The low grafting density was controlled by AFM imaging (Fig. S6) showing well-dispersed molecules on the surface. Standard approach-retraction cycles were performed using very soft cantilevers to detect small forces and small length variations of the viologen tweezers during the force-induced  $\pi$ -interaction breaking. The experiments were performed in acetonitrile (MeCN), a good solvent for the solvation of the modified viologen tweezers and the  $\pi$ -donors. The first experiments in the absence of  $\pi$ -donors showed (Fig. 2) a single-peak profile. This behavior is typical of a flexible polymer such as PEG chains and can be fitted using a statistical mechanical model—namely the worm-like chain (WLC) model.<sup>35</sup> This model relates the force exerted by the molecule to its extension and provides the persistence length value of the chain being stretched by the AFM tip, reflecting the chain flexibility. The single-peak pattern, which was adjusted automatically by the WLC model, revealed a persistence length value of  $0.3 \pm 0.05$  nm in agreement with the flexibility of a PEG chain. The rupture force corresponding to the desorption extends to values up to 150 pN, in agreement with a polymer physisorption, and is high enough to detect the intramolecular interactions of interest.<sup>23,31</sup> The rupture distance is always below 40 nm, which is

the maximum extended length of the molecule. These values are in favor of the stretching of individual molecules exhibiting the viologen tweezer component in an open form.

### ***Mechanical opening of a single viologen tweezer***

Similar approach-retraction cycles were performed in the presence of 1,5-dimethoxynaphthalene (DMNP) in MeCN. Since derivatives of dioxynaphthalene (DNP) are used<sup>12</sup> routinely as  $\pi$ -donor templates in the synthesis of MIMs, the viologen-DNP interaction force has already been characterized in one of our previous investigations<sup>31</sup> on a series of oligorotaxanes. However, in oligorotaxanes, H-bond interactions between viologen protons and the electron-rich polyethers that constitute the dumbbell also contribute to the measured rupture force. The present study is thus a unique opportunity to evaluate the contribution of both interactions in the mechanical strength detected in oligorotaxanes. In the presence of DMNP, we observe a characteristic pattern in the force-distance curves, showing a deviation from the usual single-peak profile corresponding to the desorption of the PEG linker. This pattern consists (Fig. 3A) of a first peak at about 73 pN, followed by the final desorption peak. In order to relate this pattern to the mechanical opening of the viologen tweezer, we measured the length increment ( $\Delta x$ ) at constant force after the appearance of the first peak. In other words, this  $\Delta x$  value corresponds to the length released once the D-A  $\pi$ -interaction is broken mechanically. The distribution of the length increment is shown in Fig. 3D: the most probable value is  $1.4 \pm 0.2$  nm. Considering the length difference between the closed (0.7 nm) and open (2.3 nm) forms of the viologen tweezer (distance between external pyridinium units), the experimental  $\Delta x$  value is in good agreement with the theoretical value of 1.6 nm. Additionally, the rupture force, corresponding to the  $\pi$ -interaction rupture ( $73 \pm 6$  pN) observed here (Fig. 3E) matches perfectly the value ( $72 \pm 4$  pN) obtained<sup>31</sup> recently under similar conditions (in MeCN) during the unfolding of single oligorotaxanes. Hence, we suggest that this double-peak is the signature (Fig. 1B) of the

mechanical opening of one viologen tweezer from its closed form—from encapsulating 1,5-dimethoxynaphthalene in its cavity—to its open form. We can thus also conclude that the  $\pi$ -interactions in the oligorotaxanes are the main interactions contributing to the mechanical stability, the H-bonds between the dumbbell and the rings having a minor contribution. We also observe some single-peak profiles similar to the ones obtained for the experiments without  $\pi$ -donors, corresponding to statistical events when only one part of the molecule (one PEG linker) is stretched by the AFM tip or when the  $\pi$ -donor is interacting with the viologens of the tweezer in its open form.

### ***Modulating the interaction force with different $\pi$ -donors***

In order to demonstrate the possibility of probing various weak noncovalent bonding interactions using our strategy of obtaining a force value instead of equilibrium energetic information, we selected two other compounds showing, respectively, high and low affinities with the viologen units. Firstly, we performed a similar experiment in presence of 1,5-diaminonaphthalene (DANP) in MeCN. The association constant reported<sup>12,36-37</sup> in MeCN for DMNP derivatives with the blue box is about  $3 \times 10^4 \text{ M}^{-1}$  whereas the  $K_a$  value for DANP derivatives with the blue box is slightly higher, i.e.,  $6 \times 10^4 \text{ M}^{-1}$  (Table 1). In order to compare the rupture force values, we maintained identical experimental conditions during all the SMFS experiments. These experiments in the presence of DANP showed exactly the same type of profiles as the experiments conducted with DMNP. Double-peak profiles were analyzed in the same way and returned an increment length ( $\Delta x$ ) of  $1.5 \pm 0.1 \text{ nm}$ , similar to the length obtained with DMNP and in excellent agreement with the mechanical opening of a single viologen tweezer. Remarkably, the first peak force is about 82 pN. The increase of the interaction force (Table 1) follows the increase in  $K_a$  values<sup>12,36-37</sup>, although the difference in  $K_a$  is small. This higher force detected by the AFM cantilever is a consequence of the presence of a slightly better  $\pi$ -donor hosted by the viologen tweezer.

In an attempt to assess the sensitivity of our strategy, we performed similar experiments in the presence of dimethoxybiphenyl (DMBP) in MeCN. Derivatives of dioxybiphenyl have<sup>12,38</sup> much lower association constants ( $1.4 \times 10^2 \text{ M}^{-1}$ ) with the blue box, and so we expected a significantly lower force required to break the viologen-DMBP interaction. In the event, we observed similar double-peak profiles with a revealed length ( $\Delta x$ ) of  $1.5 \pm 0.1 \text{ nm}$ , again in good agreement with the theoretical value for the opening of the viologen tweezer. The most probable peak force value is 58 pN (Table 1), which is much lower than the values observed in the cases of DMNP and DANP. The force distribution (Fig. S8) is biased due to the impossibility of detecting the additional peak at low force values. This observation is an indication that some peaks attributed to the opening of a viologen tweezer occur at much lower forces and cannot be differentiated from the inherent noise of the experiment. Again, the trend of  $K_a$  values between the  $\pi$ -donor derivatives and the blue box is maintained for the rupture force values between DMNP, DANP or DMBP, and the viologen units.

### ***In-situ $\pi$ -donor exchange***

The strength of a noncovalent bonding interaction, as well as the force required to break it, is dependent on the environment and local perturbations. In an attempt to detect the possible ejection of a  $\pi$ -donor from the viologen tweezer cavity, we designed an exchange experiment in solution. We started the standard stretching experiments in the presence of DMBP molecules (weak  $\pi$ -donors), and then we added DANP molecules (strong  $\pi$ -donors) at similar concentrations in the experimental medium (DMBP molecules were not removed). Before and after the addition of DANP, we detected similar double-peak patterns, exactly as we did in the standard experiments described previously. Figure 4 shows the distributions of peak force, i.e., the force associated with the  $\pi$ -interaction breaking, before and after the addition of DANP. We clearly observe a large shift from 50 pN (before the addition of DANP) to 84 pN (after the addition of

DANP). Before the addition, DMBP molecules are the only ones encapsulated in the closed form of the viologen tweezers, leading to low peak force values. As soon as we add the DANP molecules, the peak force increases to much higher values corresponding to the encapsulation of these strong  $\pi$ -donors. It is important to note that, after the addition of DANP molecules, we did not detect any second force population at low force values, that would have evidenced the presence of DMBP molecules still encapsulated in the viologen tweezers. We observed only a typical broadening of the distribution at higher force values. These results confirm the rapid exchange of DMBP molecules in the cavity of the viologen tweezers by DANP molecules *in situ*.

## CONCLUSIONS

The stability of noncovalent bonding interactions in terms of thermodynamic association constants or free energies are used routinely to make wholly synthetic compounds with specific functions. When it comes to describing or comparing the mechanical work performed by artificial molecular machines or motors, non-equilibrium thermodynamics applies and the relevant measure is a mechanical force. Given the vector character of force, the mechanical stability of an interaction can differ considerably from its thermodynamic stability. In this context, single-molecule force spectroscopy allows the determination of the force required to break molecular interactions. In the research described in this paper we designed and synthesized a molecular tweezer suitable for carrying out AFM-based force spectroscopy and demonstrate that we are able to quantify the mechanical strength of individual donor-acceptor  $\pi$ -interactions. Force-extension double-peak profiles reveal the mechanical opening of viologen tweezers with different  $\pi$ -donors. The rupture forces detected follow the trend observed for the  $K_a$  values with the blue box in solution.<sup>38-40</sup> *In situ* weak-to-strong  $\pi$ -donor exchange experiments also showed the sensitivity of our strategy with a clear change in force.

In summary, we are in a position to propose a simple way to measure the mechanical force of donor-acceptor  $\pi$ -interactions under similar stretching conditions. Such measurements are required for the characterization of the mechanics and operation of molecular machines, always driven out-of-equilibrium to carry out their specific tasks. It also highlights the importance of single-molecule force spectroscopy techniques for the comparison of the performance between biological and wholly synthetic molecular machines in the future.

## **ASSOCIATED CONTENT**

### **Supporting information**

The Supporting Information is available free of charge on the ACS Publications website.

Synthetic protocols and characterization, substrate preparation, AFM-based experimental details and data analysis (PDF).

## **AUTHOR INFORMATION**

### **Corresponding author**

Damien Sluysmans - UR MolSys, University of Liege, Sart-Tilman, B6a, 4000 Liege, Belgium.

Email: [damien.sluysmans@uliege.be](mailto:damien.sluysmans@uliege.be)

### **Notes**

The authors declare no competing financial interest.

## **ACKNOWLEDGMENTS**

D.S. is a Postdoctoral Researcher of the F.R.S.-FNRS (Chargé de recherches) and was supported by a Fellowship of the Belgian American Educational Foundation (B.A.E.F.). D.S. also thanks Wallonie-Bruxelles International (WBI.World) and the Vocatio Foundation for financial support. This research is part of a collaboration with Northwestern University (NU). D.S., L.Z., X.L, A.G. and J.F.S. would like to thank NU for their continued support of this research.

## REFERENCES

1. Hobza, P.; Řezáč, J. Introduction: Noncovalent Interactions. *Chem. Rev.* **2016**, *116*, 4911 – 4912.
2. Müller-Dethlefs, K.; Hobza, P. Noncovalent Interactions: A Challenge for Experiment and Theory. *Chem. Rev.* **2000**, *100*, 143 – 167.
3. Riley, K. E.; Hobza, P. Noncovalent Interactions in Biochemistry. *WIREs Comput. Mol. Sci.*, **2011**, *1*, 3 – 17.
4. Lodish, H.; Berk, A.; Zipursky, S. L.; Matsudaira, P.; Baltimore, D.; Darnell, J. *Chemical Foundations in Molecular Cell Biology*, 4<sup>th</sup> Edition, W. H. Freeman, New-York **2000**.
5. Bustamante, C.; Chemla, Y. R.; Forde, N. R.; Izhaky, D. Mechanical Processes in Biochemistry. *Annu. Rev. Biochem.* **2004**, *73*, 705 – 748.
6. Spies, M. *DNA Helicases and DNA Motor Proteins*; Springer, New-York, **2013**.
7. Balzani, V.; Credi, A.; Raymo, F. M.; Stoddart, J. F. Artificial Molecular Machines, *Angew. Chem. Int. Ed.* **2000**, *39*, 3348 – 3391.
8. Browne, W. R.; Feringa, B. L. Making Molecular Machines Work. *Nat. Nanotechnol.* **2006**, *1*, 25 – 35.
9. Kay, E. R.; Leigh, D. A.; Zerbetto, F. Synthetic Molecular Motors and Mechanical Machines. *Angew. Chem. Int. Ed.* **2007**, *46*, 72 – 191.
10. Erbas-Cakmak, S.; Leigh, D. A.; McTernan, C. T.; Nussbaumer, A. L. Artificial Molecular Machines. *Chem. Rev.* **2015**, *115*, 10081 – 10206.
11. Sluysmans, D.; Stoddart, J. F. Growing Community of Artificial Molecular Machinists. *Proc. Natl. Acad. Sci. USA.* **2018**, *115*, 9359 – 9361.
12. Bruns, C. J.; Stoddart, J. F. *The Nature of the Mechanical Bond: From Molecules to Machines*; Wiley & Sons, Inc., Hoboken, New Jersey, **2017**.

13. Sluysmans, D.; Stoddart, J. F. The Burgeoning of Mechanically Interlocked Molecules in Chemistry. *Trends Chem.* **2019**, *1*, 185 – 197.
14. Barin, G.; Coskun, A.; Fouda, M. M. G.; Stoddart, J. F. Mechanically Interlocked Molecules Assembled by  $\pi$ - $\pi$  Recognition. *ChemPlusChem* **2012**, *77*, 159 – 185.
15. Emmett, L.; Prentice, G. M.; Pantos, G. D. Donor-Acceptor Interactions in Chemistry. *Annu. Rep. Prog. Chem., Sct. B: Org. Chem.*, **2013**, *109*, 217 – 234.
16. Hoffmann, P. M. *Life's Ratchet: How Molecular Machines Extract Order from Chaos*; Basic Books, New-York, **2012**.
17. Astumian, R. D. Irrelevance of the Power Stroke for the Directionality, Stopping Force, and Optimal Efficiency of Chemically Driven Molecular Machines. *Biophys. J.* **2015**, *108*, 291 – 303.
18. Astumian, R. D.; Mukherjee, S.; Warshel, A. The Physics and Physical Chemistry of Molecular Machines. *Chemphyschem* **2016**, *17*, 1719 – 1741.
19. Pezzato, C.; Cheng, C.; Stoddart, J. F.; Astumian, R. D. Mastering the Non-Equilibrium Assembly and Operation of Molecular Machines. *Chem. Soc. Rev.* **2017**, *46*, 5491 – 5507.
20. de Souza, N. Pulling on Single Molecules. *Nat. Methods* **2012**, *9*, 873 – 877.
21. Neuman, K.; Nagy, A. Single-Molecule Force Spectroscopy: Optical Tweezers, Magnetic Tweezers and Atomic Force Microscopy. *Nat. Methods* **2008**, *5*, 491 – 505.
22. Duwez, A.-S.; Willet, N. *Molecular Manipulation with Atomic Force Microscopy*; CRC Press, **2012**.
23. Clausen-Schaumann, H.; Seitz, M. ; Krautbauer, R. ; Gaub, H. E. Force Spectroscopy with Single Bio-Molecules. *Curr. Opin. Chem. Biol.* **2000**, *4*, 524 – 530.

24. Scholl, Z. N.; Li, Q.; Marszalek, P. E. Single Molecule Mechanical Manipulation for Studying Biological Properties of Proteins, DNA, and Sugars. *WIREs Nanomed Nanobiotechnol* **2014**, *6*, 211 – 229.
25. Fisher, T. E.; Marszalek, P. E.; Fernandez, J. M. Stretching Single Molecules into Novel Conformations using the Atomic Force Microscopy. *Nat. Struct. Biol.* **2000**, *7*, 719 – 724.
26. Puchner, E. M.; Gaub, H. E. Force and Function : Probing Proteins with AFM-based Force Spectroscopy. *Curr. Opin. Struct. Biol.* **2009**, *19*, 605 – 614.
27. Gardini, L.; Tempestini, A.; Pavone, F. S.; Capitanio, M. High-Speed Optical Tweezers for the Study of Single Molecular Motors. In: Lavelle, C. (eds) *Molecular Motors. Methods in Molecular Biology*, vol. 1805. Humana Press, New-York, NY, **2018**.
28. Lussis, P.; Svaldo-Lanero, T.; Bertocco, A.; Fustin, C.-A.; Leigh, D. A.; Duwez, A.-S. A Single Synthetic Small Molecule that Generates Force Against a Load. *Nat. Nanotechnol.* **2011**, *6*, 553 – 557.
29. Van Quaethem, A.; Lussis, P.; Leigh, D. A.; Duwez, A.-S.; Fustin, C.-A. Probing the Mobility of Catenane Rings in Single Molecules. *Chem. Sci.* **2014**, *5*, 1449 – 1452.
30. Naranjo, T.; Lemishko, K. M.; de Lorenzo, S.; Somoza, A.; Ritort, F.; Pérez, E.; Ibarra, B. Dynamics of Individual Molecular Shuttles under Mechanical Force. *Nat. Commun.* **2018**, *9*, 4512 – 4518.
31. Sluysmans, D.; Hubert, S.; Bruns, C. J.; Zhu, Z.; Stoddart, J. F.; Duwez, A.-S. Synthetic Oligorotaxanes Exert High Forces when Folding under Mechanical Load. *Nat. Nanotechnol.* **2018**, *13*, 209 – 213.
32. Sluysmans, D.; Devaux, F.; Bruns, C. J.; Stoddart, J. F.; Duwez, A.-S. Dynamic Force Spectroscopy of Synthetic Oligorotaxane Foldamers. *Proc. Natl. Acad. Sci. USA* **2018**, *115*, 9362 – 9366.

33. Odell, B.; Reddington, M. V.; Slawin, A. M. Z.; Spencer, N.; Stoddart, J. F.; Williams, D. J. Cyclobis(paraquat-*p*-phenylene). A Tetracationic Multipurpose Receptor. *Angew. Chem. Int. Ed.* **1988**, *27*, 1547 – 1550.
34. Sluysmans, D.; Willet, N.; Thevenot, S.; Lecommandoux, S.; Duwez, A.-S. Single-Molecule Mechanical Unfolding Experiments Reveal a Critical Length for the Formation of Alpha-Helices in Peptides. *Nanoscale Horiz.* **2020**, *5*, 671 – 678.
35. Marantan, A.; Mahadevan, L. Mechanics and Statistics of the Worm-Like Chain. *Am. J. Phys.* **2018**, *86*, 86 – 94.
36. Choi, J. W.; Flood, A. H.; Steuerman, D. W.; Nygaard, S.; Braunschweig, A. B.; Moonen, N. N. P.; Laursen, B. W.; Luo, Y.; DeIonno, E.; Peters, A. J.; Jeppesen, J. O.; Xu K.; Stoddart, J. F.; Heath, J. R. Ground-State Equilibrium Thermodynamics and Switching Kinetics of Bistable [2]Rotaxanes Switched in Solution, Polymer Gels, and Molecular Electronic Devices. *Chem. Eur. J.* **2006**, *12*, 261 – 279.
37. Sue, C.-H.; Basu, S.; Fahrenbach, A. C.; Shveyd, A. K.; Dey, S. K.; Botros, Y. Y.; Stoddart, J. F. Enabling Tetracationic Cyclophane Production by Trading Templates. *Chem. Sci.* **2010**, *1*, 119 – 125.
38. Córdova, E.; Bissell, R. A.; Spencer, N.; Ashton, P. R.; Stoddart, J. F.; Kaifer, A. Novel Rotaxanes Based on the Inclusion Complexation of Biphenyl Guests by Cyclobis(paraquat-*p*-phenylene). *J. Org. Chem.* **1993**, *58*, 6550 – 6552.

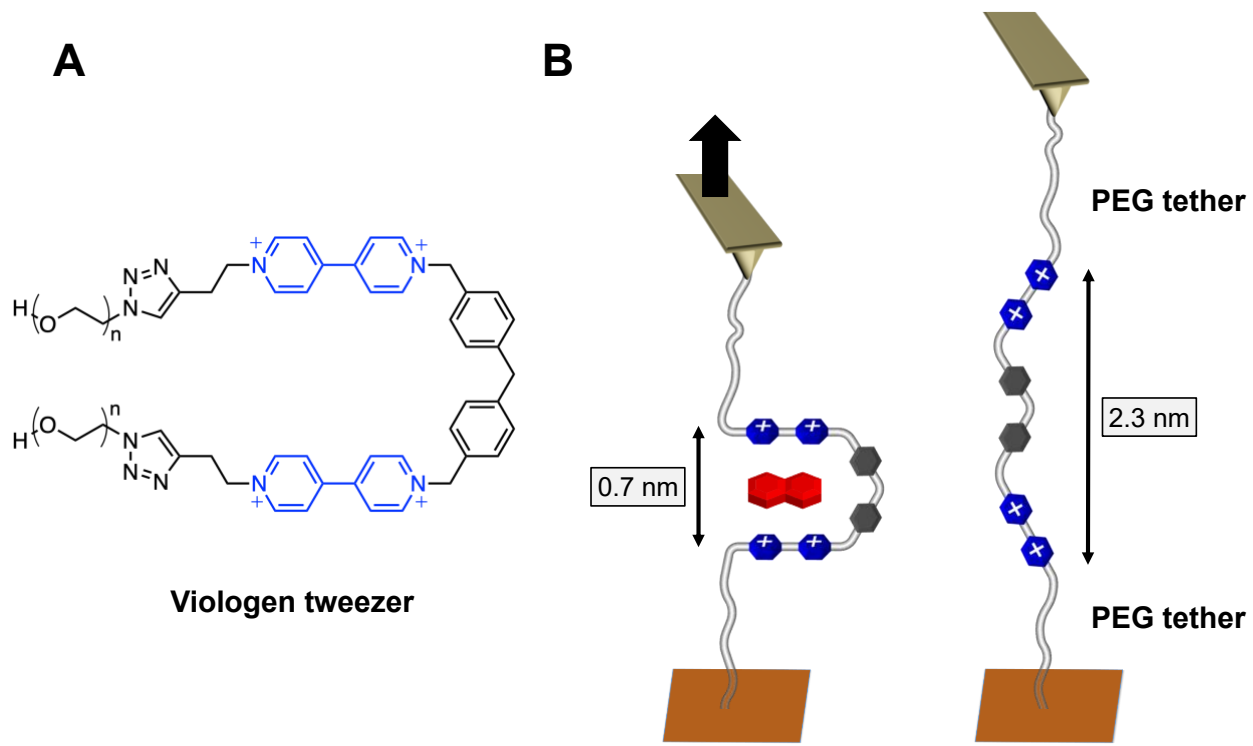
## CAPTIONS AND FIGURES

**Figure 1.** Structural formula of the viologen tweezer (A) and a scheme of the AFM force spectroscopy experiment (B). The viologen tweezer, modified with PEG tethers, is trapped between an AFM tip and a mica substrate. The tip is pulled away from the surface and the forces applied on the close (B, *left*) and opened (B, *right*) forms are measured. The  $\pi$ -donor is represented in red. Information about the distances between the viologen units are given in the SI.  $\text{PF}_6^-$  Counterions are not represented.

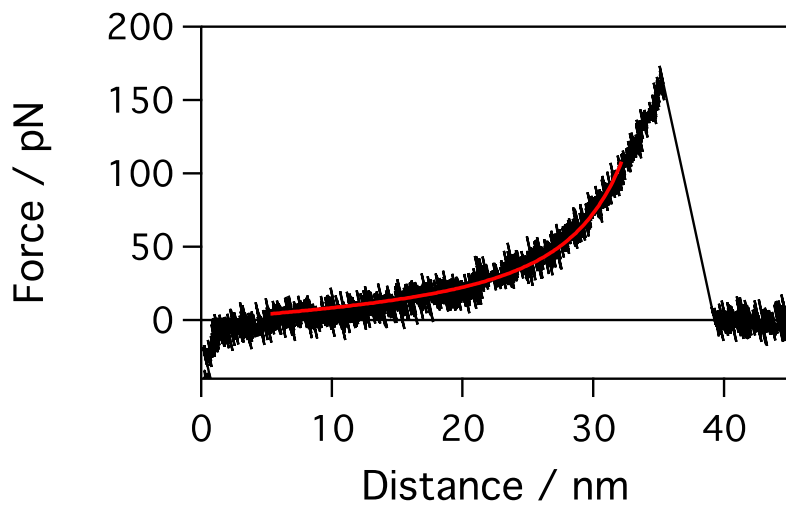
**Figure 2.** Pulling experiment performed on the viologen tweezers in MeCN in the absence of  $\pi$ -donors. The force-distance profile illustrates the typical stretching of a flexible linear polymer, based on a worm-like chain (WLC) model (fit in red).

**Figure 3.** Pulling on the viologen tweezers in presence of  $\pi$ -donors. (A,B,C) Typical force-distance curves (with WLC fits in red) showing a second peak in presence of 1,5-dimethoxynaphthalene (DMNP, A), 1,5-diaminonaphthalene (DANP, B) or dimethoxybiphenyl (DMBP, C). (D) Distribution of the length increment between the first and the second peak, measured at constant force in presence of DMNP. The Gaussian fit (in red) affords  $\Delta x = 1.4 \pm 0.2$  nm. PDF Distribution is added in dotted line. (E) Distribution of peak force, i.e., first peak in force curve A, with a Gaussian fit (in red) giving  $F_{peak} = 73 \pm 6$  pN. PDF distribution is added in dotted line.

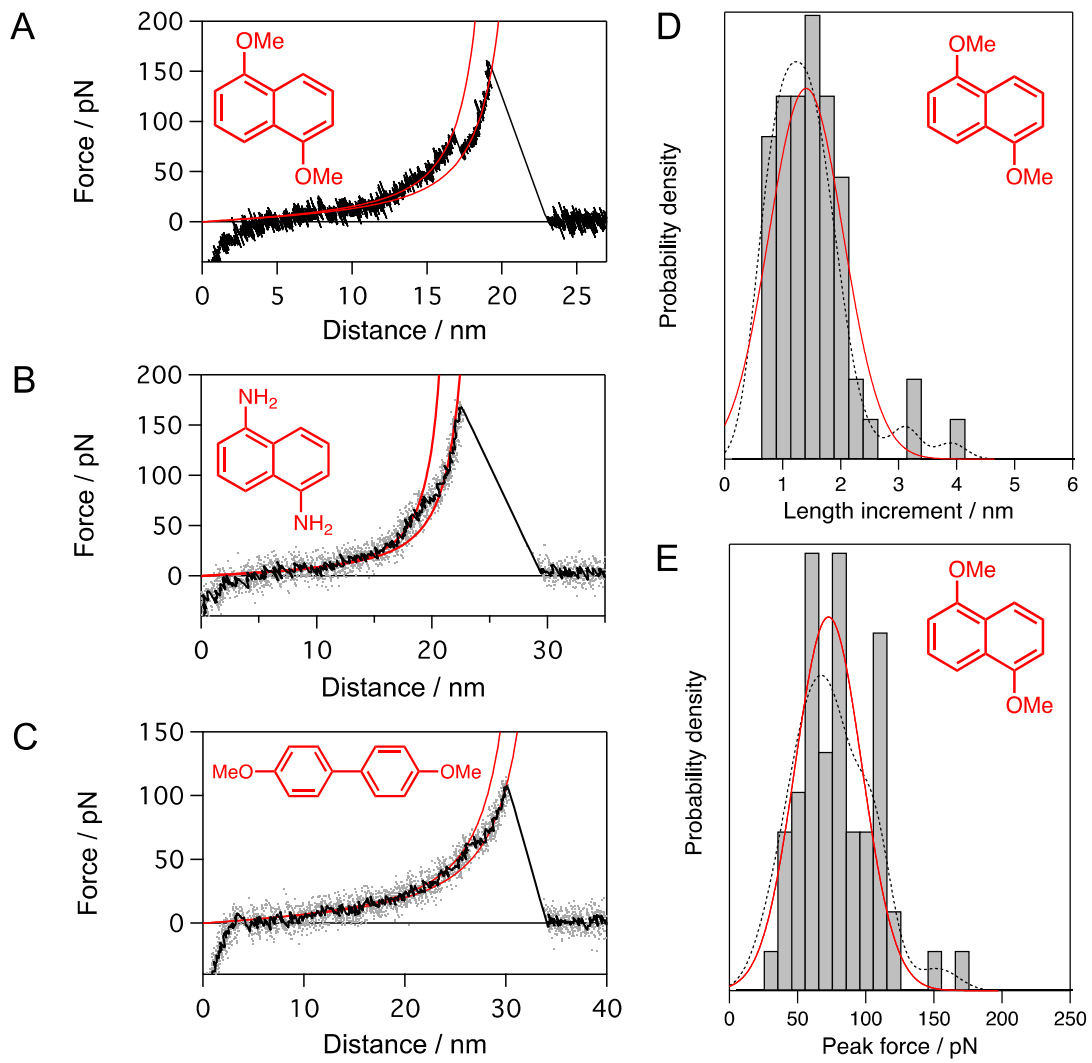
**Figure 4.** Distributions of the force of the first peak for double-peak profiles in exchange experiments, before (green) and after (blue) addition of DANP. Histograms are superimposed with associated Gaussian fits on the data, giving  $F_{peak} = 50 \pm 7$  and  $84 \pm 10$  pN, respectively, before and after the addition of DANP. A clear change in force is observed corresponding to the exchange of the weak DMBP  $\pi$ -donor by the strong DANP  $\pi$ -donor within the viologen tweezer cavity.



**Figure 1**



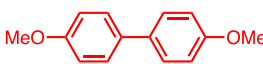
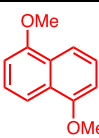
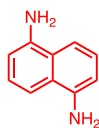
**Figure 2**



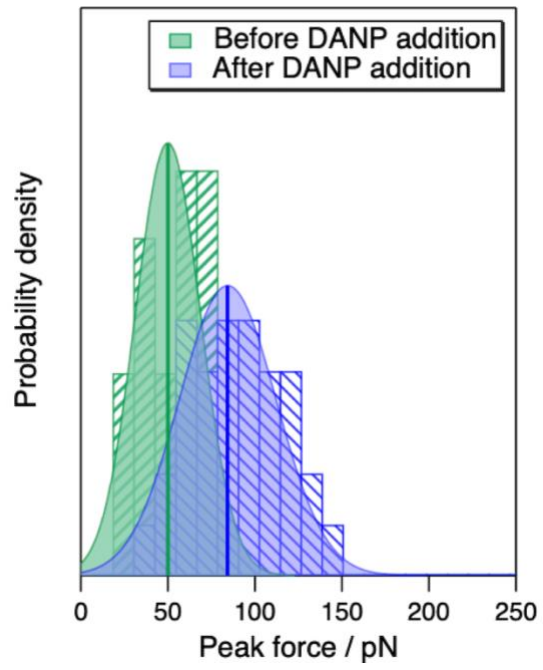
**Figure 3**

**Table 1**

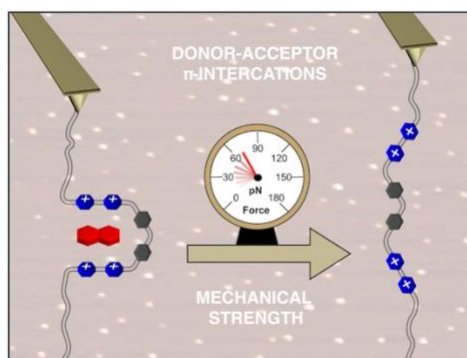
(Left) Association constant between  $\pi$ -donors and the blue box.<sup>12,36-38</sup> (Right) Values of length increment ( $\Delta x$ ) and  $\pi$ -interaction force ( $F_{peak}$ ) determined by SMFS for various  $\pi$ -donors in the cavity of the viologen tweezer.

$\pi$ -Donor derivative	$K_a$ with blue box / mol <sup>-1</sup>	$\pi$ -Donor	$\Delta x$ / nm	$F_{peak}$ / pN
Dioxybiphenyl	$\sim 10^2$		$1.5 \pm 0.1$	$58 \pm 7$
Dioxynaphthalene	$\sim 3 \times 10^4$		$1.4 \pm 0.2$	$73 \pm 6$
Diaminonaphthalene	$\sim 6 \times 10^4$		$1.5 \pm 0.1$	$82 \pm 6$

Experimental  $\Delta x$  values are in agreement with theoretical revealed length during the mechanical opening of the viologen tweezer. The trend observed for the peak force is consistent with  $K_a$  values for  $\pi$ -donors.



**Figure 4**



For Table of Contents Only